Research Paper

Pharmacokinetic Characteristics of Bisdemethoxycurcumin and Its Mechanism of Reversing Cardiomyocyte Apoptosis

WEI LIU, JING XIAN[1], JIAN WANG[1], JINGSHUANG HUANG[1] AND ZONGKAI XU[1]*

Department of Biotechnology, Sichuan Center for Food and Drug Evaluation, Inspection and Monitoring, [1]C-Luminary Biotechnology Co., Ltd., Chengdu, Sichuan 610000, China

To investigate the pharmacokinetic characteristics of bisdemethoxycurcumin *in vivo* and the reversal effect of phosphatidylinositol 3-kinase/protein kinase B/caspase-9 signaling pathway on thapsigargin-induced cardiomyocyte apoptosis in neonatal rat. Demethoxycurcumin and bisdemethoxycurcumin were intragastrically administered to adult Sprague–Dawley rats. Plasma was collected and the drug concentration was measured by high performance liquid chromatography. The pharmacokinetic parameters of the drug were calculated by Drug and Statistics 2.1.1 pharmacokinetic software. After that, primary cardiomyocytes from Sprague–Dawley neonatal rats were isolated and cultured, and they were divided into three groups; control (conventional culture without any drug treatment), model (endoplasmic reticulum stress model obtained by treatment with 1 mg/ml thapsigargin for 24 h), demethoxy curcumin group (treated with 1 µmol/l thapsigargin and 10 µmol/l demethoxy curcumin for 24 h at the same time) and bisdemethoxycurcumin group (treated with 1 µmol/l thapsigargin and 10 µmol/l bisdemethoxycurcumin for 24 h at the same time). Cell survival activity was measured by cell counting kit-8 assay. Western blot was used to detect the expression of intracellular apoptotic factors Bcl-2-associated X, B-cell lymphoma protein 2 and B-cell lymphoma protein 2/Bcl-2-associated X protein and the expression levels of phosphatidylinositol 3-kinase/protein kinase B/caspase-9 signaling pathway molecules phosphatidylinositol 3-kinase, protein kinase B, caspase-3 and caspase-9 protein. The results showed that the main pharmacokinetic parameters area under the time-concentration curve 0-12 h, mean residency time 0-12 h, maximum plasma concentration, time to maximum plasma concentration of demethoxycurcumin and bisdemethoxycurcumin were (1.35±0.36) µg/ml•h and (1.01±0.14) µg/ml•h, (4.05±0.53) h and (3.43±0.21) h, (0.46±0.09) µg/ml and (0.45±0.11) µg/ml, (0.14±0.00) h and (0.20±0.00) h, respectively. In contrast with the model group, the survival activity of demethoxycurcumin and bisdemethoxycurcumin groups was significantly increased, the apoptosis rate was significantly decreased; the lactate dehydrogenase, malondialdehyde content and reactive oxygen species level were decreased, the superoxide dismutase activity was increased, the Bcl-2-associated X, caspase-3 and caspase-9 protein expression was decreased and the B-cell lymphoma protein 2/Bcl-2-associated X, phosphatidylinositol 3-kinase and protein kinase B protein expression was increased ($p<0.05$). However, bisdemethoxycurcumin was slightly superior to demethoxycurcumin in improving the above indicators, but the difference was not statistically meaningful ($p>0.05$). In summary, demethoxy curcumin and bisdemethoxycurcumin can mediate phosphatidylinositol 3-kinase/protein kinase B/caspase-9 signaling pathway to reduce thapsigargin-induced endoplasmic reticulum stress injury in cardiomyocytes, which in turn plays a protective role in cardiomyocytes.

Key words: Demethoxycurcumin, bisdemethoxycurcumin, pharmacokinetics, cardiomyocyte, endoplasmic reticulum, stress

Turmeric has the functions of activating blood circulation to remove blood stasis, relieving pain and detumescence[1]. Turmeric has been widely used in the clinical treatment of dysmenorrhea, rheumatic arthralgia and thoracic obstruction, and has played an excellent therapeutic effect[2]. Curcumin (CC), Demethoxycurcumin (DC) and Bisdemethoxycurcumin (BC) are the main active components of turmeric, which have similar chemical

***Address for correspondence**
E-mail: zhingxuzongkai@163.com

structure and pharmacological effects[3]. It has been confirmed that CC is able to exert a protective effect against cardiovascular injury and it can be used in the treatment of diseases such as atherosclerosis[4,5]. However, the *in vivo* pharmacokinetics of CC is not stable, so it can't be widely used in clinical practice. DC and BC, which are similar derivatives of CC, can also exert similar pharmacological effects and have more stable chemical characteristics, so they are safe in metabolism *in vivo*[6]. However, there is a lack of studies on the protective effects and mechanisms of DC and BC on cardiomyocytes.

Numerous studies have confirmed that myocardial cells undergo massive apoptosis under the stimulation of cardiac injury, which is an important mechanism responsible for the development and progression of cardiac diseases[7,8]. Apoptosis refers to the behavior of cells to induce their own programmed death under the stimulation of adverse factors. The pathways leading to apoptosis are the mitochondrial apoptosis pathway, the death ligand-death receptor pathway and the Endoplasmic Reticulum (ER) stress pathway[9].

In cells, the ER is a crucial subunit structure involved in intracellular protein post-synthetic modification, folding and secretion, lipid metabolism and other functions[10]. The ER homeostasis and function of cells are disrupted under pathological conditions, resulting in the misfolding or accumulation of intracellular proteins, which triggers ER stress, whereas persistent stress conditions can lead to a dysfunctional ER misfolding protein stress response and damages appear, leading to cell apoptosis[11]. Phosphatidylinositol 3-Kinase (PI3K)/Protein Kinase B (AKT) signaling pathway is involved in cell survival, growth and apoptosis. It has been confirmed that regulating the PI3K/AKT signaling pathway, is able to slow down the apoptotic process of cardiomyocytes, followed by exerting a protective effect against cardiac injury[12,13]. The caspase family includes two categories; caspase-3, an executioner of apoptosis and caspase-9, an initiator of apoptosis, which are target proteins downstream of AKT and are involved in the apoptosis pathway[14]. The regulation of PI3K/AKT/caspase-9 is the key to effectively inhibit cardiomyocyte apoptosis.

The pharmacokinetic properties and *in vitro* drug release behavior of free DC and BC medicines were compared. Thapsigargin (TG) was used to induce neonatal rat cardiomyocytes and prepare an ER stress injury model to explore the mechanism by which DC and BC regulated PI3K/AKT/caspase-9 signaling pathway to inhibit cardiomyocyte apoptosis. The aim was to provide an objective basis for the in-depth exploration of clinical pharmacodynamics, as well as the research and development of drugs for the prevention and treatment of cardiovascular diseases.

MATERIALS AND METHODS

Experiment reagent:

DC (purity >98 %) and BC (purity >98 %) were purchased from Tokyo Chemical Industry Co., Ltd. Male adult healthy Sprague-Dawley (SD) rats, (88±3) d, weighing (245±15) g; SD neonatal rats (24~48) h were purchased from the Animal Experimental Center of Zhejiang Chinese Medical University. TG was purchased from Sigma, United States of America (USA). Lactate Dehydrogenase (LDH), Malondialdehyde (MDA) and Superoxide Dismutase (SOD) detection kits were purchased from Nanjing Jiancheng Bioengineering Company. Reactive Oxygen Species (ROS) detection kit, Bicinchoninic Acid (BCA) assay protein quantitative detection kit and Enhanced Chemiluminescence (ECL) detection kit were purchased from Beyotime Biotechnology. Rabbit polyclonal antibody PI3K (ab154598), rabbit polyclonal antibody AKT (ab38449), rabbit monoclonal antibody caspase-3 (ab184787), rabbit monoclonal antibody caspase-9 (ab184786), rabbit monoclonal antibody Bcl-2 Associated X-Protein (BAX) (ab182733), rabbit polyclonal antibody B-Cell Lymphoma 2 (Bcl-2) (ab196495) and rabbit anti-rat Immunoglobulin G (IgG) H&L (Horseradish Peroxidase (HRP)) secondary antibody (ab6734) were purchased from Abcam.

In vivo pharmacokinetic analysis:

Male adult SD rats were adaptively fed for 3 d, fasted 12 h before administration and intragastrically administered with 200 mg/kg DC and BC raw material medicines, respectively. At 0 h, 0.25 h, 0.5 h, 1 h, 3 h, 6 h and 12 h after administration, blood was collected from the orbital venous plexus. After heparin sodium anticoagulant treatment, it was placed in a water bath at 37° for 20 min and centrifuged at 3500 rpm for 10 min. The supernatant was taken to calculate the drug concentration in plasma and the drug-time curve was plotted to calculate the pharmacokinetic parameters.

Culture and grouping of neonatal rat cardiomyocytes:

Myocardial tissue was taken from the apex of neonatal rats under aseptic conditions and divided into blocks of 1 mm^3 using disinfected surgical scissors. 0.15 % trypsin solution was added, the blocks were digested in a water bath at 37° and made into cardiomyocyte suspension and subsequently centrifuged at 1000 rpm for 10 min. Dulbecco's Modified Eagle's Medium (DMEM) containing 15 % fetal bovine serum was added to the precipitation and the cell concentration was adjusted to 1×10^6 cells and seeded in cell culture flasks for primary culture. After 24 h of routine culture, it was replaced with serum-free DMEM medium for another 24 h and the cells were randomly divided as follows.

Control group: Primary cardiomyocytes were not treated with any drugs and routine culture was performed for 24 h.

Model group: 1 µmol/l TG reagent was added to primary cardiomyocytes and routinely cultured for 24 h.

DC group: 1 µmol/l TG reagent and 10 µmol/l DC solutions were added to primary cardiomyocytes and routinely cultured for 24 h.

BC group: Primary cardiomyocytes were added with 1 µmol/l TG reagent and 10 µmol/l BC solution and routinely cultured for 24 h.

Detection of cell survival rate by Cell Counting Kit-8 (CCK-8):

The concentration of primary cardiomyocytes obtained by isolation was adjusted to 5×10^4 cells/ml and seeded in 96-well plates. The cells were treated in groups and cultured for 6 h. The cells were washed with Phosphate Buffered Saline (PBS) and 10 µl of CCK-8 reagent was added to each well for 2 h. The wells without cells and reagents were set as blank wells, the wells with reagents were set as control wells and the wells with cells and reagents were set as test wells. The absorbance of each well was detected at a wavelength of 450 nm using a multifunctional Ultraviolet (UV) spectrophotometer. The cell survival rate was calculated

$$\text{Survival rate } (\%)=(OD_{experiment}-OD_{blank})/(OD_{control}-OD_{blank})\times100\ \%\ (1)$$

Detection of apoptosis by flow cytometry:

Detection of apoptosis rate was performed according to the Annexin V-Fluorescein Isothiocyanate (V-FITC)/Propidium Iodide (PI) double staining method. Primary cardiomyocytes were routinely cultured and processed in groups, cells were digested with 0.2 % trypsin and cell precipitation were collected by centrifugation at 1000 rpm for 10 min. Cells were washed adopting precooled PBS reagent, centrifuged at 1000 rpm for 10 min and then suspended by adding 500 µl Annexin V Binding buffer. Subsequently, 5 µl of Annexin V-FITC reagent was added and it was mixed well, protected from light and incubated at room temperature for 15 min. 5 µl PI reagent was added for staining 5 min before being put on the machine and the wavelength of FITC emission light was 515 nm and that of PI emission light was 560 nm. The detection of apoptosis rate was subsequently performed adopting flow cytometry and the relative quantification of apoptosis was performed using flow Jo software.

Detection of LDH, MDA and SOD levels in cells:

Primary cardiomyocytes were seeded at a concentration of 1×10^6 cells/ml in 6-well plates and treated in groups for 6 h of regular culture. Cells were collected to make a homogenate solution and intracellular markers were measured according to the LDH, MDA and SOD detection kits instructions. In the steps of MDA detection, myocardial cells and reagents were added in turn and it was vortexes well, in a boiling water bath at 95° for 40 min and centrifuged at 4000 rpm for 10 min. The supernatant was taken to determine the absorbance of cells in each well at wavelengths of 450 nm, 532 nm and 450 nm using a multifunctional UV spectrophotometer and the LDH, MDA and SOD contents were calculated.

Detection of ROS level in cells:

Primary cardiomyocytes were seeded in 96-well plates at a concentration of 5×10^4 cells/ml and processed in groups for routine culture for 6 h. The measurement of intracellular ROS levels in each group was performed according to the ROS assay kit instructions. ROS fluorescent probes were added to cardiomyocytes to reach a final concentration of 10 µmol/l. It was incubated at 37° for 1 h. ROS levels in the cells of each group were detected at a wavelength of 500 nm/530 nm using a full-wavelength micro plate reader.

Detection of target protein expression by Western blot:

The treated cells from each group were collected and Radioimmunoprecipitation Assay (RIPA) lysate was added to fully lyse the cells on ice. Quantitative detection of protein concentration was performed using the BCA assay kit and the sample protein concentration was adjusted to 30 μg. The sample proteins were subjected to Sodium Dodecyl-Sulfate Polyacrylamide Gel Electrophoresis (SDS-PAGE) at voltages of 80 V and 120 V. Proteins were transferred to Polyvinylidene Difluoride (PVDF) membranes adopting the semi-dry transfer method with a transfer time of about 90 min. Blocking treatments were performed for 2 h using Phosphate-Buffered Saline with 0.1% Tween® 20 (TBST) blocking solution containing 5 % non-fat dry milk, followed by addition of 1:1000 diluted primary antibody and incubation at 4° overnight. After washing the membranes with TBST, 1:2000 diluted secondary antibodies was added and it was incubated at room temperature for 2 h. ECL chemical emission detection kit was used for emission detection and gel imaging system was adopted for exposure. Beta-actin (β-actin) was used as an internal reference gene to quantitatively detect the PI3K, AKT, caspase-3, caspase-9, Bcl-2 and BAX protein expression.

Statistical processing:

Statistical Package for the Social Sciences (SPSS) 19.0 software was adopted for statistical processing and analysis of the test data. All the result data were expressed as mean±Standard Deviation (SD). The difference was statistically analyzed by one-way Analysis of Variance (ANOVA) process. $p<0.05$ suggested there was statistically meaningful.

RESULTS AND DISCUSSION

Blank plasma, internal standard fluid+plasma (1:10) adult SD rats were taken and the plasma of rats was analyzed by High-Performance Liquid Chromatography (HPLC) after gavage of BC or DC. The results are shown in fig. 1. A standard solution of 0.015 μg/ml~5 μg/ml was prepared. After plotting the chromatogram, it was found that the standard curve of BC drug was; A=3.2311C+0.0309, R^2=0.9998; the standard curve of DC drug was; A=3.0162C+0.2831, R^2=0.9995.

The findings of SD rats treated with BC and DC were plotted as a plasma concentration-time curve, as shown in fig. 2. About 3 h after gavage, the plasma concentration peaked and then steadily dropped. The trends of plasma concentration-time curves of BC and DC were basically the same.

The differences of pharmacokinetic parameters between SD rats treated with BC and DC were compared. The results are shown in fig. 3. The Area Under Curve (AUC_{0-12h}) of BC and DC were (1.01±0.14) μg/ml•h, (1.35±0.36) μg/ml•h; Mean Residency Time (MRT_{0-12h}) were (3.43±0.21) h, (4.05±0.53) h; maximum plasma Concentration (C_{max}) were (0.45±0.11) μg/ml, (0.46±0.09) μg/ml; Time to maximum plasma concentration (T_{max}) were (0.20±0.00) h and (0.14±0.00) h, respectively.

CCK-8 assay was used to detect the difference of cardiomyocyte viability in each group (fig. 4). The viability of myocardial cells in the control, model, DC and BC groups was (98.59±5.14) %, (28.62±5.09) %, (79.71±6.17) % and (85.97±4.43) %.

Compared with the control group, the viability of myocardial cells in the model, DC and BC groups was significantly decreased ($p<0.05$). Relative to the model group, the viability of myocardial cells in the DC and BC groups was significantly increased ($p<0.05$).

Flow cytometry was used to detect the difference of cardiomyocyte apoptosis rate among groups (fig. 5). The cardiomyocyte apoptosis rates of control, model, DC and BC groups were (2.16±0.44) %, (19.78±1.21) %, (5.56±1.07) % and (4.03±0.89) %.

The apoptosis rate of cardiomyocytes in the model, DC and BC groups was obviously increased ($p<0.05$). The apoptosis rate of cardiomyocytes in DC and BC groups was clearly decreased ($p<0.05$).

The differences of LDH, MDA and SOD levels in neonatal rat cardiomyocytes were detected by kit (fig. 6). The LDH levels were (19.03±1.56) IU/l, (65.17±2.37) IU/l, (30.63±2.15) IU/l and (28.94±2.09) IU/l, MDA levels were (8.23±1.13) nmol/ml, (29.97±2.56) nmol/ml, (16.43±1.31) nmol/ml and (15.56±1.44) nmol/ml, SOD levels were (35.62±3.09) nU/ml, (14.56±2.81) nU/ml, (26.70±2.33) nU/ml and (28.82±1.89) nU/ml in the control, model, DC and BC groups, respectively.

The levels of LDH and MDA were significantly increased and the level of SOD was significantly decreased ($p<0.05$) in the model, DC, BC groups. The levels of LDH and MDA in myocardial cells were significantly decreased and the level of SOD was significantly increased in the DC and BC groups ($p<0.05$).

The difference of ROS levels in neonatal rat cardiomyocytes was detected and compared by the kit (fig. 7). The levels of ROS in control, model, DC and BC groups were (0.56±0.21), (7.71±1.07), (2.31±0.43) and (1.89±0.50) respectively.

The levels of ROS in myocardial cells in the model, DC and BC groups were significantly increased ($p<0.05$). The level of ROS in myocardial cells in the DC and BC groups was significantly decreased ($p<0.05$).

The levels of apoptotic factors BAX and Bcl-2 in neonatal rat cardiomyocytes of each group were detected by Western blot and Bcl-2/BAX was calculated (fig. 8). The expression of BAX protein, Bcl-2 protein and Bcl-2/BAX of cells in control, model, DC and BC groups was (0.79±0.14), (1.62±0.18), (1.10±0.08), (1.08±0.22); (1.15±0.16), (0.33±0.08), (0.72±0.21), (0.89±0.23) and (0.24±0.02), (0.06±0.1), (0.11±0.04), (0.14±0.03).

The expression of BAX was obviously increased and the expression of Bcl-2 and the ratio of Bcl-2/BAX were obviously decreased in the myocardial cells of the model group, DC and BC groups ($p<0.05$). The expression of BAX was clearly decreased, and the expression of Bcl-2 and Bcl-2/BAX ratio were obviously increased in the DC and BC groups ($p<0.05$).

Western blot was used to detect the differences in the expression of PI3K, AKT, caspase-3 and caspase-9 proteins in neonatal rat cardiomyocytes (fig. 9). The expression of PI3K protein was (1.65±0.18), (0.41±0.08), (1.04±0.13) and (1.10±0.20), the expression of AKT protein was (1.43±0.22), (0.80±0.14), (1.12±0.25) and (1.21±0.27), the expression of caspase-3 was (0.45±0.11), (1.15±0.23), (0.72±0.18) and (0.63±0.24) and the expression of caspase-9 was (0.53±0.17), (1.22±0.2), (0.72±0.09) and (0.64±0.15) in control, model, DC and BC groups.

The expression of PI3K and AKT proteins in myocardial cells was significantly decreased, and the expression levels of caspase-3 and caspase-9 proteins were significantly increased in the model, DC and BC groups ($p<0.05$). The expression of PI3K and AKT proteins in myocardial cells was obviously increased and the expression of caspase-3 and caspase-9 proteins was clearly decreased ($p<0.05$) in the DC and BC groups.

The major ingredients in traditional Chinese medicine turmeric are CC compounds. CC has been shown in studies to lessen the severity of myocardial ischemia-reperfusion injury following a myocardial infarction, hence protecting heart function[15]. Others have confirmed that CC can reduce the severity of diabetes-

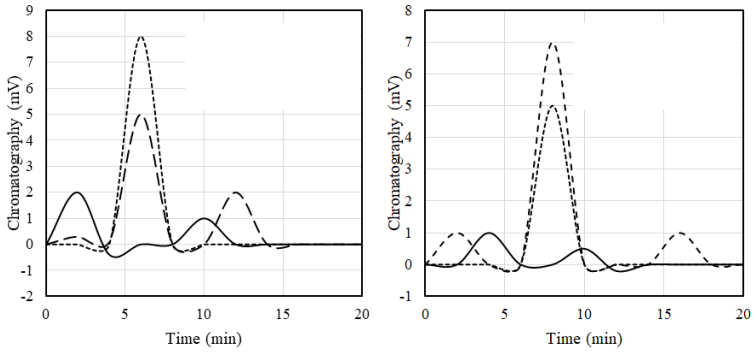

Fig. 1: HPLC chromatogram analysis
Note: (———): Blank plasma; (- - - - - - -): Internal standard and (— — -): BC

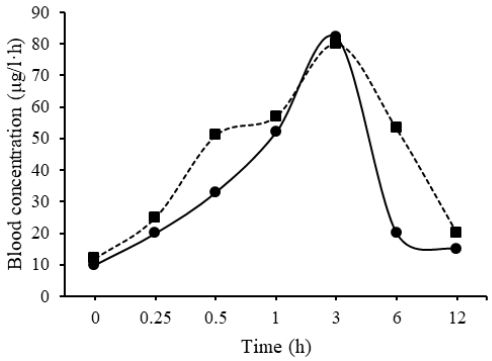

Fig. 2: Plasma concentration curve after intragastric administration of DC and BC
Note: (—●—): BC and (--■--): DC

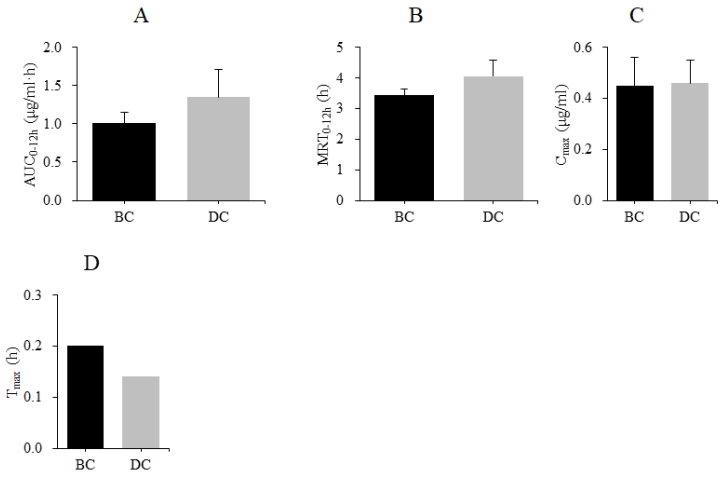

Fig. 3: Pharmacokinetic parameters of DC and BC
(A): Area under the curve (AUC); (B): Mean residence time (MRT); (C): C_{max} and (D): T_{max}

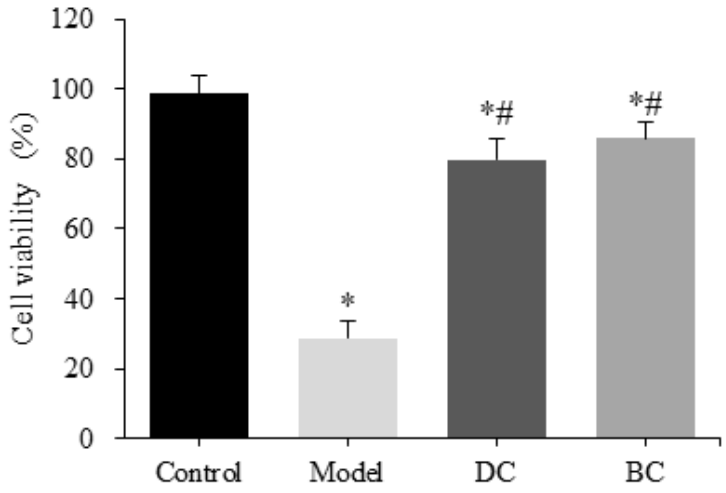

Fig. 4: Detection of myocardial cell viability in neonatal rats
Note: Compared with the control group, *p<0.05 and compared with the model group, #p<0.05

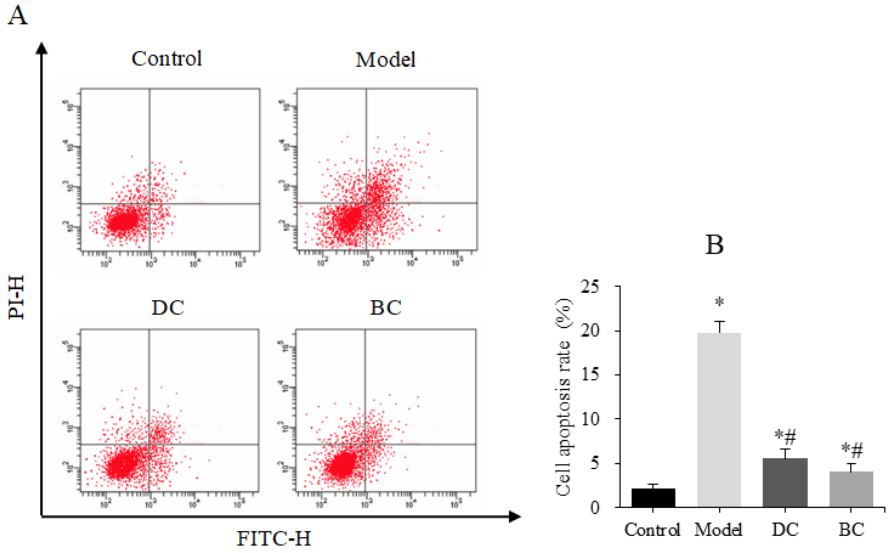

Fig. 5: Detection of cardiomyocyte apoptosis rate in neonatal rats, (A): The flow cytometry diagram and (B): Apoptosis rate calculation
Note: Compared with the control group, *p<0.05 and compared with the model group, #p<0.05

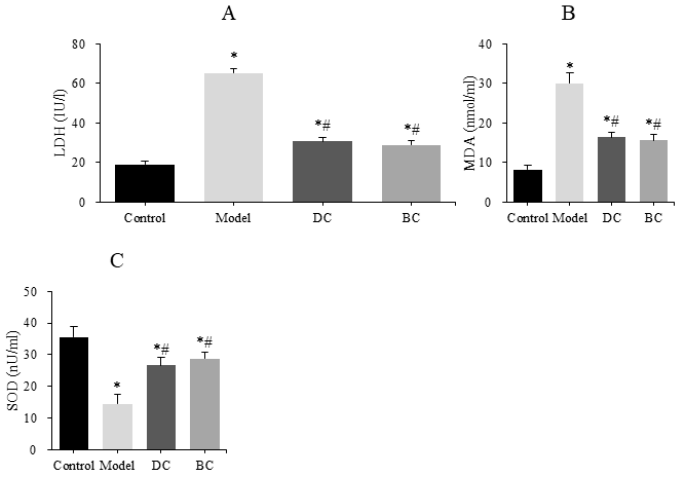

Fig. 6: Detection of LDH, MDA and SOD levels in neonatal rat cardiomyocytes, (A): LDH level; (B): MDA level and (C): SOD level
Note: Compared with the control group, *p<0.05 and compared with the model group, #p<0.05

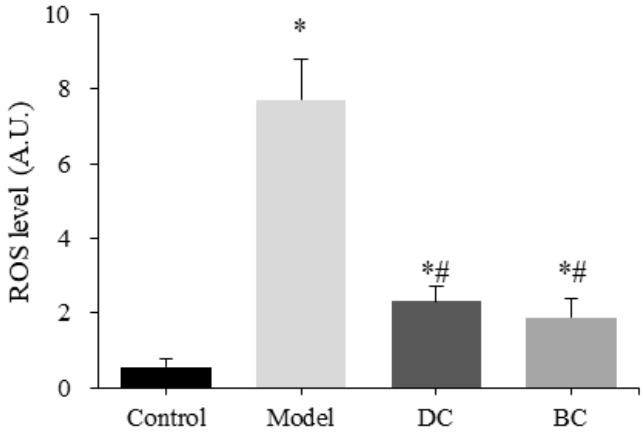

Fig. 7: Detection of ROS level in neonatal rat cardiomyocytes
Note: Compared with the control group, *p<0.05 and compared with the model group, #p<0.05

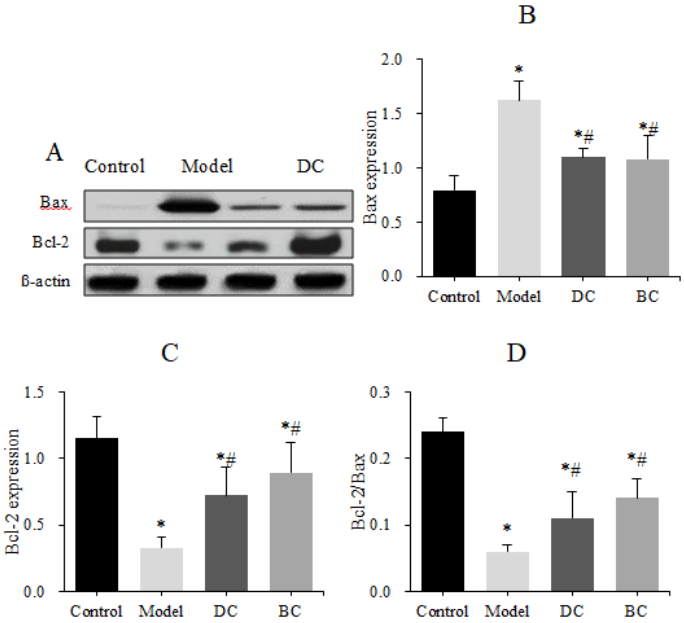

Fig. 8: Detection of BAX, Bcl-2 protein expression and Bcl-2/BAX ratio in neonatal rat cardiomyocytes, (A): Western blot detection map; (B): Relative expression of BAX protein; (C): Relative expression of Bcl-2 protein and (D): Bcl-2/BAX ratio
Note: Compared with the control group, *p<0.05 and compared with the model group, #p<0.05

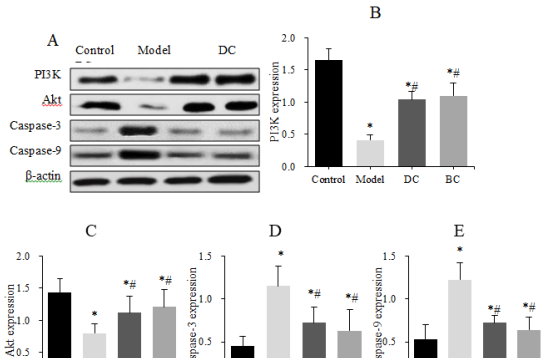

Fig. 9: Detection of PI3K, AKT, caspase-3 and caspase-9 protein expression in neonatal rat cardiomyocytes. (A): Western blot detection map; (B): Relative expression of PI3K protein; (C): Relative expression of AKT protein; (D): Relative expression of caspase-3 protein and (E): Relative expression of caspase-9 protein

Note: Compared with the control group, *p<0.05 and compared with the model group, #p<0.05

related cardiac damage[16]. However, CC is easily oxidized and can be easily decomposed by light, so it can't be widely used in clinical practice. BC is a natural derivative of CC, which possesses the same mother nucleus structure as CC and has similar pharmacological activity[17].

Compared with CC as well as DC, BC is a highly selective competitive inhibitor of human aldehyde-ketone reductase 1B10[18]. Studies have confirmed that the nuclear cell uptake ability and stability of BC drugs are significantly higher than those of CC[19]. It showed that BC has a good development prospect as a therapeutic agent for the disease. The *in vivo* drug release and pharmacokinetic characteristics of DC and BC drugs were analyzed. The *in vivo* release profiles of DC and BC drugs were similar and there was no significant difference; there were slight differences in the pharmacokinetics parameters $AUC_{0\text{-}12h}$, $MRT_{0\text{-}12h}$, C_{max} and T_{max} between the two types of drugs, DC drugs had shorter time to peak and longer circulation time *in vivo*, but the difference was not statistically significant. The findings revealed that both DC and BC exhibited high bioavailability, laying the groundwork for further research into their mechanisms of action on cardiomyocyte apoptosis. Cardiomyocyte apoptosis is an important pathological feature of ischemic heart disease and inhibition of myocardial apoptosis can significantly improve cardiac function[20]. Apoptosis resulting from ER stress injury in cardiomyocytes is mediated by three ER transmembrane protein kinase R-like ER kinases, activated transcription factor 6, as well as inositol enzyme 1[21].

Prolonged exposure of cells to ER stress promotes apoptosis and is involved in the progression of a variety of cardiovascular diseases[22]. TG is often used for the preparation of cellular ER stress injury models, mainly by inhibiting intracellular calcium pump and Magnesium (Mg^{2+}) ions-Adenosine Triphosphate (ATPase), so that a large amount of Calcium (Ca^{2+}) ions is transported into the cytoplasm, and the decrease of Ca^{2+} level in the ER will lead to its dysfunction, which in turn causes the misfolding or accumulation of intracellular proteins and finally triggers ER stress injury in cells[23]. TG was used to induce ER stress injury model in neonatal rat cardiomyocytes. Cardiomyocyte activity was dramatically reduced, although apoptosis rate was significantly enhanced, intracellular LDH and MDA contents were increased and SOD activity was lowered, according to the findings. LDH is widely present in human tissues, mainly distributed in the kidney, heart muscle and skeletal muscle. Studies have confirmed that LDH levels increase significantly when myocardial injury occurs[24]. MDA and SOD are important parameters to reflect the anti-oxidative stress ability of the body, which can reflect the rate and intensity of lipid peroxidation[25]. It has been confirmed that MDA levels are significantly increased, while SOD activity is significantly decreased when myocardial injury is induced by ischemia-reperfusion in the body[26]. ROS are signaling molecules necessary for cell growth and excess ROS is a major factor leading to oxidative stress in cells[27]. Among the oxidative stresses in cells, mitochondrial dysfunction, ER stress and cytoplasmic membrane peroxidation are all causes of multi-site and multi-effect damage in cells[28]. The results showed that intracellular ROS levels were significantly increased in cardiomyocytes after TG induction. It showed that a cardiomyocyte apoptosis model induced by ER stress injury was successfully prepared. Clinically, the Nuclear Factor Erythroid 2-related factor 2 (Nrf2) agonist dimethyl fumarate is mostly used for the treatment of multiple sclerosis diseases, while plant extracts such as sulforaphane, CC, as well as mistletoe are also able to activate Nrf2

by alkylation or covalent modification. While TG induced ER stress injury model in cardiomyocytes, it was found that after administration of DC and BC drugs, the myocardial cell activity was significantly increased, the apoptosis rate was significantly decreased, the intracellular LDH and MDA contents were reduced, the SOD activity was increased and the ROS level was significantly decreased. The regulation of apoptosis pathways is dependent on the balance of anti-apoptotic protein Bcl-2 and pro-apoptotic protein BAX[29,30]. After TG induction, the expression of BAX protein was dramatically elevated in cardiomyocytes, while the expression of Bcl-2 protein and the Bcl-2/BAX ratio were significantly lowered. It was found that BAX expression level decreased, Bcl-2 and Bcl-2/BAX increased in cardiomyocytes after DC and BC treatment, indicating that DC and BC have a good antioxidant effect, can reduce the oxidative stress level of TG-induced myocardial ER stress injury and inhibit apoptosis. Studies have confirmed that the activation of PI3K/AKT signaling pathway, is able to participate in the process of apoptosis inhibition, which in turn slows down the process of heart failure[31]. Among the caspase family molecules, caspase-3 belongs to the executor of apoptosis, caspase-9 belongs to the initiator of apoptosis and both caspase-3 and caspase-9 are target proteins downstream of AKT in the PI3K/AKT pathway, which can regulate apoptosis after cleaving Deoxyribonucleic Acid (DNA) by destroying the cytoskeleton of cells[32,33]. The results revealed that after treatment with DC and BC, the expression of PI3K and AKT proteins was significantly increased, while the expression of caspase-3 and caspase-9 proteins was significantly decreased in the TG-induced cardiomyocyte ER injury model. It indicated that DC and BC could activate the PI3K/AKT signaling pathway in cardiomyocytes, reduce the expression of caspase-9 after activating AKT and then inhibit the cascade of caspase, so that downstream caspase-3 was no longer activated and then play a role in inhibiting apoptosis and alleviating the process of cardiomyocyte injury.

The goal was to look at the pharmacokinetic differences between DC and BC medicines *in vivo*, as well as their inhibitory effects on apoptosis induced by TG-induced ER stress damage in cardiomyocytes. There was no significant variation in pharmacokinetic parameters between DC and BC medicines and they had good bioavailability, according to the findings. However, in the ER stress injury model induced by TG treated with DC and BC, the cell survival activity was increased, the apoptosis rate was decreased, the LDH, MDA content and ROS level were decreased, the SOD activity was increased, the BAX, caspase-3 and caspase-9 proteins expression levels were decreased and the Bcl-2, Bcl-2/BAX, PI3K and AKT protein expression levels were increased. DC and BC can inhibit the expression of apoptotic molecules in TG-induced ER stress injury model of cardiomyocytes by activating PI3K/AKT signaling pathway and improve the level of oxidative stress, followed by inhibition of apoptosis. However, only the effects of DC and BC-free pharmaceuticals were studied and future research will focus on the therapeutic effects of drug nano-emulsion formulations in order to extend the medication's *in vivo* release period. Animal models will be prepared to verify the protective effects of DC and BC drugs on myocardial injury induced by heart disease *in vivo*. It aims to provide experimental materials for the development of new therapeutic drugs for cardiac diseases.

Conflict of interests:

The authors declared no conflict of interests.

REFERENCES

1. Giordano A, Tommonaro G. Curcumin and cancer. Nutrients 2019;11(10):2376.
2. Mansouri K, Rasoulpoor S, Daneshkhah A, Abolfathi S, Salari N, Mohammadi M, *et al.* Clinical effects of curcumin in enhancing cancer therapy: A systematic review. BMC Cancer 2020;20(1):791.
3. Liu J, Wang Q, Omari-Siaw E, Adu-Frimpong M, Liu J, Xu X, *et al.* Enhanced oral bioavailability of Bisdemethoxycurcumin-loaded self-microemulsifying drug delivery system: Formulation design, *in vitro* and *in vivo* evaluation. Int J Pharm 2020;590:119887.
4. Ashtary-Larky D, Rezaei Kelishadi M, Bagheri R, Moosavian SP, Wong A, Davoodi SH, *et al.* The effects of nano-curcumin supplementation on risk factors for cardiovascular disease: A GRADE-assessed systematic review and meta-analysis of clinical trials. Antioxidants 2021;10(7):1015.
5. Salehi B, Del Prado-Audelo ML, Cortés H, Leyva-Gómez G, Stojanović-Radić Z, Singh YD, *et al.* Therapeutic applications of curcumin nanomedicine formulations in cardiovascular diseases. J Clin Med 2020;9(3):746.
6. Huang C, Lu HF, Chen YH, Chen JC, Chou WH, Huang HC. Curcumin, demethoxycurcumin and bisdemethoxycurcumin induced caspase-dependent and–independent apoptosis *via* Smad or Akt signaling pathways in HOS cells. BMC Complement Med Ther 2020;20(1):68.
7. Tocchetti CG, Ameri P, de Boer RA, D'Alessandra Y, Russo M, Sorriento D, *et al.* Cardiac dysfunction in cancer patients: Beyond direct cardiomyocyte damage of anticancer drugs: Novel cardio-oncology insights from the joint 2019 meeting of the esc working groups of myocardial function and cellular biology of the heart. Cardiovasc Res 2020;116(11):1820-34.
8. Jones JL, Peana D, Veteto AB, Lambert MD, Nourian Z, Karasseva NG, *et al.* TRPV4 increases cardiomyocyte calcium cycling and contractility yet contributes to damage in the aged heart following hypoosmotic stress. Cardiovasc Res 2019;115(1):46-56.

9. Nakada Y, Nhi Nguyen NU, Xiao F, Savla JJ, Lam NT, Abdisalaam S, *et al.* DNA damage response mediates pressure overload–induced cardiomyocyte hypertrophy. Circulation 2019;139(9):1237-9.
10. Gurunathan S, Kang MH, Jeyaraj M, Kim JH. Palladium nanoparticle-induced oxidative stress, endoplasmic reticulum stress, apoptosis and immunomodulation enhance the biogenesis and release of exosome in human leukemia monocytic cells (THP-1). Int J Nanomed 2021;16:2849-77.
11. Sisinni L, Pietrafesa M, Lepore S, Maddalena F, Condelli V, Esposito F, *et al.* Endoplasmic reticulum stress and unfolded protein response in breast cancer: The balance between apoptosis and autophagy, and its role in drug resistance. Int J Mol Sci 2019;20(4):857.
12. Song HP, Chu ZG, Zhang DX, Dang YM, Zhang Q. PI3K–AKT pathway protects cardiomyocytes against hypoxia-induced apoptosis by MitoKATP-mediated mitochondrial translocation of pAKT. Cell Physiol Biochem 2018;49(2):717-27.
13. Li Y, Xia J, Jiang N, Xian Y, Ju H, Wei Y, *et al.* Corin protects H_2O_2-induced apoptosis through PI3K/AKT and NF-κB pathway in cardiomyocytes. Biomed Pharmacother 2018;97:594-9.
14. Kumar D, Haldar S, Gorain M, Kumar S, Mulani FA, Yadav AS, *et al.* Epoxyazadiradione suppresses breast tumor growth through mitochondrial depolarization and caspase-dependent apoptosis by targeting PI3K/Akt pathway. BMC Cancer 2018;18(1):52.
15. Saeidinia A, Keihanian F, Butler AE, Bagheri RK, Atkin SL, Sahebkar A. Curcumin in heart failure: A choice for complementary therapy? Pharmacol Res 2018;131:112-9.
16. Sudirman S, Lai CS, Yan YL, Yeh HI, Kong ZL. Histological evidence of chitosan-encapsulated curcumin suppresses heart and kidney damages on streptozotocin-induced type-1 diabetes in mice model. Sci Rep 2019;9(1):15233.
17. Incha MR, Thompson MG, Blake-Hedges JM, Liu Y, Pearson AN, Schmidt M, *et al.* Leveraging host metabolism for bisdemethoxycurcumin production in *Pseudomonas putida*. Metab Eng Commun 2020;10:e00119.
18. Jin F, Chen X, Yan H, Xu Z, Yang B, Luo P, *et al.* Bisdemethoxycurcumin attenuates cisplatin-induced renal injury through anti-apoptosis, anti-oxidant and anti-inflammatory. Eur J Pharmacol 2020;874:173026.
19. Ramezani M, Hatamipour M, Sahebkar A. Promising anti-tumor properties of bisdemethoxycurcumin: A naturally occurring curcumin analogue. J Cell Physiol 2018;233(2):880-7.
20. Liu Z, Xu Y, Wan Y, Gao J, Chu Y, Li J. Exosomes from adipose-derived mesenchymal stem cells prevent cardiomyocyte apoptosis induced by oxidative stress. Cell Death Discov 2019;5(1):1-7.
21. Ren L, Wang Q, Chen Y, Ma Y, Wang D. Involvement of microRNA-133a in the protective effect of hydrogen sulfide against ischemia/reperfusion-induced endoplasmic reticulum stress and cardiomyocyte apoptosis. Pharmacology 2019;103(1-2):1-9.
22. Yan M, Chen K, He L, Li S, Huang D, Li J. Uric acid induces cardiomyocyte apoptosis *via* activation of calpain-1 and endoplasmic reticulum stress. Cell Physiol Biochem 2018;45(5):2122-35.
23. Oakes SA. Endoplasmic reticulum stress signaling in cancer cells. Am J Pathol 2020;190(5):934-46.
24. Chen C, Cong BL, Wang M, Abdullah M, Wang XL, Zhang YH, *et al.* Neutrophil to lymphocyte ratio as a predictor of myocardial damage and cardiac dysfunction in acute coronary syndrome patients. Integr Med Res 2018;7(2):192-9.
25. Amin MM, Rafiei N, Poursafa P, Ebrahimpour K, Mozafarian N, Shoshtari-Yeganeh B, *et al.* Association of benzene exposure with insulin resistance, SOD and MDA as markers of oxidative stress in children and adolescents. Environ Sci Pollution Res 2018;25(34):34046-52.
26. Bai M, Pan CL, Jiang GX, Zhang YM, Zhang Z. CircHIPK3 aggravates myocardial ischemia-reperfusion injury by binding to miRNA-124-3p. Eur Rev Med Pharmacol Sci 2019;23(22):10107-14.
27. Cadenas S. ROS and redox signaling in myocardial ischemia-reperfusion injury and cardioprotection. Free Radic Biol Med 2018;117:76-89.
28. Khezri S, Sabzalipour T, Jahedsani A, Azizian S, Atashbar S, Salimi A. Chrysin ameliorates aluminum p hosphide-induced oxidative stress and mitochondrial damages in rat cardiomyocytes and isolated mitochondria. Environ Toxicol 2020;35(10):1114-24.
29. Wu H, Zhu H, Zhuang Y, Zhang J, Ding X, Zhan L, *et al.* LncRNA ACART protects cardiomyocytes from apoptosis by activating PPAR-γ/Bcl-2 pathway. J Cell Mol Med 2020;24(1):737-46.
30. Mohamed AA, Khater SI, Arisha AH, Metwally MM, Mostafa-Hedeab G, El-Shetry ES. Chitosan-stabilized selenium nanoparticles alleviate cardio-hepatic damage in type 2 diabetes mellitus model *via* regulation of caspase, Bax/Bcl-2 and Fas/FasL-pathway. Gene 2021;768:145288.
31. Zhang L, Guo Z, Wang Y, Geng J, Han S. The protective effect of kaempferol on heart *via* the regulation of Nrf2, NF-κβ and PI3K/Akt/GSK-3β signaling pathways in isoproterenol-induced heart failure in diabetic rats. Drug Dev Res 2018;80(3):294-309.
32. Ayoup MS, Fouad MA, Abdel-Hamid H, Abu-Serie MM, Noby A, Teleb M. Battle tactics against MMP-9; discovery of novel non-hydroxamate MMP-9 inhibitors endowed with PI3K/AKT signaling attenuation and caspase 3/7 activation *via* Ugi bis-amide synthesis. Eur J Med Chem 2020;186:111875.
33. Yuan J, Deng Y, Zhang Y, Gan X, Gao S, Hu H, *et al.* Bmp4 inhibits goose granulosa cell apoptosis *via* PI3K/AKT/caspase-9 signaling pathway. Anim Reprod Sci 2019;200:86-95.

This article was originally published in a special issue, "Role of Biomedicine in Pharmaceutical Sciences" Indian J Pharm Sci 2023:85(2) Spl Issue "64-73"